A major purpose of the Technical Information Center is to provide the broadest dissemination possible of information contained in DOE's Research and Development Reports to business, industry, the academic community, and federal, state and local governments.

Although a small portion of this report is not reproducible, it is being made available to expedite the availability of information on the research discussed herein.

1

LA-UR-83-3505

LA-UR--83-3505

DE84 004334

CONF-831205--47

Los Alamos National Laboratory is operated by the University of California for the United States Department of Energy under contract W-7405-ENG-36

TITLE PLASMA ENGINEERING DESIGN OF A COMPACT REVERSED-FIELD PINCH REACTOR (CRFPR)

AUTHOR(S) C. G. Bathke, M. J. Embrechts, R. L. Hagenson
R. A. Krakowski, and R. L. Miller

SUBMITTED TO to be presented at 10th Symposium on Fusion Engineering, Philadelphia, PA (December 5-9, 1983)

Los Alamos Los Alamos National Laboratory
Los Alamos, New Mexico 87545

PLASMA ENGINEERING DESIGN OF A COMPACT REVERSED-FIELD PINCH REACTOR (CRFPR)*

C. G. Bathke, M. J. Embrechts**, R. L. Hagenson***, R. A. Krakowski, R. L. Miller
Los Alamos National Laboratory
Los Alamos, NM 87545

ABSTRACT

The rationale for and the characteristics of the high-power-density Compact Reversed-Field Pinch Reactor (CRFPR) are discussed. Particular emphasis is given to key plasma engineering aspects of the conceptual design, including plasma operations, current drive, and impurity/ash control by means of pumped limiters or magnetic divertors. A brief description of the Fusion-Power-Core integration is given.

I. INTRODUCTION

Early projections[1] of Reversed-Field-Pinch (RFP) reactors were based on plasma confinement by superconducting magnets. This design approach led to systems of low engineering power density, not unlike those being projected for the mainline and other alternative fusion concepts[2,3]. Based on arguments summarized in Ref. 3, serious problems related to device development, plant operations, and end-product economics may arise because of the inefficient use of fusion-power-core (FPC, i.e., first-wall/blanket/shield/coil, FW/B/S/C) volume and mass. The compact RFP reactor (CRFPR) concept and design approach was suggested[4] and developed[5,6] to address directly these power-density issues. An option for magnetic-confinement fusion is provided with a FPC power density that can be as high as values considered economically necessary for other nuclear power systems (10-15 MWt/m^3 for LWRs, compared to 0.3-0.5 MW/m^3 for low-power-density fusion systems). Table I compares key engineering and cost parameters being projected for the compact and low-power-density (mainline) concepts to highlight essential differences.

If the RFP is to achieve the advantages of a compact reactor, a better understanding of key plasma physics/engineering processes is needed. The impact of transport scaling (startup, ignition, burn sustenance), impurity/ash control (pumped limiter versus magnetic divertors), and steady-state (non-inductive) plasma current drive influence strongly the practicality of long-pulsed or steady-state plasma operation considered as an ideal goal for the compact reactor. The physics models used to describe and project these crucial engineering processes are only beginning to emerge for the RFP, as is a more coherent picture of the minimum-energy RFP state in general. This paper, therefore, focusses onto the CRFPR plasma physics/engineering to relate present understanding to the technology projected as necessary for the ideal CRFPR limit suggested in Table I.

II. CONFINEMENT PRINCIPLE

The RFP, compact toroids (CTs, i.e., spheromaks or field-reversed configurations (FRCs)), and the tokamak confine plasma by a combination of externally applied toroidal field, B_ϕ, and self-generated poloidal fields, B_θ, resulting from toroidal currents, I_ϕ, flowing in a torus of major radius R_T and minor radius r_p. The physics successes of the tokamak member of this pinch group rest primarily with the strong "backbone" provided to the plasma by the dominant toroidal field; serious reactor limitations, however, are also imposed by the use of strong toroidal fields. Unlike the tokamak, where $B_\phi/B_\theta = q(R_T/r_p) > 10$, q being the Kruskal-Shafranov safety factor, RFPs and CTs operate with $B_\phi \approx B_\theta$ and $q < 1$, with q actually reversing sign at the plasma edge for the RFP. The reversal of B_ϕ at the plasma edge also generates high shear for stability to local MHD modes and the possibility for high-beta plasmas. An electrically conducting shell provides stability to MHD modes with wavelengths on the order of r_p. Since the $q(r_p) > 2$-3 limit does not apply to the RFP, I_ϕ is not constrained by MHD considerations, and ohmic heating to ignition may be possible.

These characteristics result in a high-beta plasma that is stably confined primarily by strong self-currents, this plasma being surrounded by an engineering structure (FPC) that need not accommodate auxiliary heating or a strong magnetic field. These features together admit the unique combination of increased plasma power density and first-wall neutron loading [I_w(MW/m^2) $\approx (\beta B^2)^2 r_p/2$], low-field blankets [thin, high-power-density (100-200 MWt/m^3, peak); liquid-metal-cooled with acceptable pressure, MHD pressure drop, and pumping power], and low-field magnetic coils [exo-blanket; low forces, mass, ohmic losses, and recirculating power], all of which are necessary for the compact reactor.[3]

Central to the achievement of these significant benefits is the formation and sustainment of a plasma/field configuration in which $B_\phi(r > r_p)$ is small (i.e., zero for spheromak, slightly reversed for the RFP) relative to $B_\phi(r = 0)$. Classically, such a configuration is expected to decay resistively on a few-second diffusion timescale at reactor conditions (shorter timescales at lower temperatures). Numerous RFP (and, more recently, spheromak) experiments have demonstrated a sustainment or "dynamo" mechanism that operates to maintain the configuration over many resistive diffusion times.

The existence of a grossly-stable and regenerative (i.e., "dynamo"-sustained) RFP configuration after passage through a turbulent, dissipative phase prompted Taylor[9,10] to describe this process as a resistive relaxation of the plasma/field configuration that conserves the total toroidal flux, Φ, and magnetic helicity, $K = \int \vec{A}\cdot\vec{B}\, dV_p = 2\psi\Phi$, where ψ is the poloidal flux, V_p is the plasma volume, and $\vec{A} = \nabla\times\vec{B}$ is the vector potential. In the case of the RFP, K measures the degree to which toroidal flux is linked by poloidal flux. Describing the relaxed, minimum-energy state as force-free [$\nabla\times\vec{B} = \mu_o\vec{J} = \mu(r)\vec{B}$] results in the Bessel-Function Model (BFM) when the scalar $\mu(r)$ is independent of plasma radius [$B_\phi = J_0(\mu r)$, $B_\theta = J_1(\mu r)$]. Defining the "Pinch Parameter," $\theta = B_\theta(r_w)/\langle B_\phi\rangle = \mu_o I_\phi r_w/2\Phi$, where $\Phi = \langle B_\phi\rangle\pi r_w^2$ is the initial toroidal flux, it follows that $\mu = 2\theta/r_w$ for the constant-μ BFM. The "Reversal Parameter," $F = B_\phi(r_w)/\langle B_\phi\rangle$ combines with θ to give a convenient description of the Taylor minimum-energy states; for

---

* Work performed under the auspices of the US DOE.
** Rensselaer Polytechnic Institute
*** Technology International, Inc.

the zero-beta, constant-μ BFM, $F = \theta J_0(2\theta)/J_1(2\theta)$, which is shown in Fig. 1 and gives the locus of minimum-energy states as constrained by the Taylor model (i.e., constant μ, ϕ, and K).

The spatially-constant μ profiles assumed for the BFM requires high current density in the region of the cold, resistive plasma edge. Modifications to the BFM generally allow for constant-μ profiles out to a radius αr_w ($\alpha < 1$), with μ decreasing continuously to zero from αr_w to r_w. Figure 1 also gives the locus of relaxed RFP states for a number of modified BFMs. Generally, theory indicates improved stability for $\theta > 1.2$, and experiment shows improved heating and confinement in the RFP region of Fig. 1. It is noted that the spheromak state is given by $F = 0$ on Fig. 1, and the tokamak-like region occurs for $F = 1$ and $\theta > 1/q(R_T/r_p)$.

The Taylor F-θ diagram demonstrates a remarkable coupling between poloidal-field (PF) and toroidal-field (TF) circuits through the plasma dynamo for both spheromak and RFP configurations; strong coupling for the tokamak does not exist. The F-θ relationship can be used to describe the RFP or spheromak plasma as a non-linear rectifying element; the possibility to maintain I_ϕ against resistive decay by in-phase oscillations of TF and PF circuits is predicated. This potential for non-inductive current drive by low-frequency and low-amplitude "F-θ pumping" adds another strong reactor advantage of a dynamo-sustained plasma contained stably by self-currents. These features as reflected in the plasma engineering of the CRFPR are now discussed.

III. PLASMA ENGINEERING

The underlying principle of RFP confinement is based on a free-energy-driven dynamo, possibly originating from $n = 1$, multiple-n-number ($n \sim 12$) resistive instabilities. The added plasma turbulence will undoubtedly increase plasma transport losses; careful attention must be given to minimizing flux and energy loss, with the plasma dynamo action being optimized during the startup transient towards an ohmically-heated DT ignition. Secondly, the low-q, high-shear flux surfaces near the B_ϕ reversal layer must be accommodated by any pumped-limiter or magnetic divertor ash/impurity control scheme. Thirdly, long-pulsed or steady-state operation must consider efficient, dynamo-based F-θ pumping. This section examines the CRFPR design in relationship to projected needs for the three following areas: plasma operations (transport, start-up, ignition/burn, etc.); ash/impurity control; and steady-state current drive. Table II gives the key plasma parameters, and Fig. 2 gives the reactor cross-section for the design being considered.[5,6]

A. Plasma Operations

Central to any description of the RFP startup is the plasma particle/energy loss, as embodied in a global energy confinement time, τ_E. A completely physics-based transport scaling does not exist for RFPs, nor is one required for the design of an ignited DT-fueled fusion reactor. Given a specific ignition parameter, $n\tau_E$, and a fusion-neutron first-wall loading, l_w, as dictated by total power, size, lifetime, heat-transfer, and economic constraints, the average plasma density, n, is determined; the global energy confinement time is then dictated solely by these techno-economic considerations under the assumption that the required plasma density (pressure) can be held by achievable values of βB^2 at the plasma surface. This economically-optimum confinement time, $\tau_E(OPT) = [(n\tau)^2 \langle\sigma v\rangle E_N/8L_w]^{1/2} r_p^{1/2}$, has been determined for the CRFPR by an extensive parameter search and optimization to be 0.25-0.30 s, a value that must be reconciled with scaled physics results.

With the usual definitions of $\mu_o = 4\pi(10)^{-7}$ H/m and $k_B = 1.602(10)^{-16}$ J/keV, pressure balance and the definition of τ_E for an ohmically-heated plasma gives, respectively

$$T(\text{keV}) = \frac{\mu_o}{16\pi k_B}\left[\frac{I_\phi}{N}\right]\beta_\theta I_\phi \tag{1}$$

$$\tau_E = \frac{3nk_BT}{nj_\phi^2} = \frac{3}{16}\mu_o\beta_\theta r_p^2\sigma, \tag{2}$$

where the last equality combines pressure and energy balance, $\sigma = 1/\eta$ is the RFP plasma electrical conductivity, $j_\phi = I_\phi/\pi r_p^2$, and the streaming parameter $I_\phi/N = j_\phi/n$ has been introduced with $N = \pi n r_p^2$ being the plasma line density. For a fixed streaming parameter and poloidal beta, β_θ, the plasma temperature is expected to scale linearly with plasma current, and $\tau_E \propto I_\phi^{3/2} r_p^2$ for a plasma conductivity that itself scales classically ($\sigma \propto T^{3/2}$). This scaling has been observed on a number of RFP experiments[11,12] in the ranges I_ϕ = 50-100 kA and $r_p \sim 0.1$-0.2 m. Also, for fixed I_ϕ/N, Eq. (1) predicts $T/I_\phi = \beta_\theta$; a comparison of RFPs with ohmically-heated tokamaks of similar current and size would show a better performance for the latter; improved RFP performance requires higher currents because of the lower poloidal beta, β_θ being close to the total beta for RFPs.

Attributing the energy loss in RFPs to anomalous electron conduction, a fit to ZT-40M data ($\tau_{ce} = 0.2$ ms, $\beta_\theta = 0.1$-0.15, $I_\phi = 0.12$ MA, $r_p = 0.2$ m) gives a $\tau_{ce} \propto I_\phi^\nu r_p^2$ scaling, where ν is in the range 0.9 - 1.5. Specifically, two limiting scaling laws emerge from experiment for use in the reactor plasma simulations.

$$\tau_{ce} = \begin{cases} 0.05\ I_\phi r_p^2 f_1(\beta_\theta) \\ 0.14\ I_\phi^{3/2} r_p^2 f_2(\beta_\theta), \end{cases} \tag{3}$$

where the functions $f_j(\beta_\theta)$ are chosen to decrease τ_{ce} as a critical values of beta, $\beta_{\theta c} = 0.13$, is exceeded, and I_ϕ has units of MA. Typically, $f_1(\beta_\theta)$ equals unity for $\beta_\theta < \beta_{\theta c}$, and $(\beta_{\theta c}/\beta_\theta)^2$ otherwise, as indicated by neutral-beam-heated tokamaks; $f_2(\beta_\theta) = \exp[2.303(1 - \beta_\theta/\beta_{\theta c})]$ is designed to reduce τ_{ce} even more rapidly as the approach to ignition tends to drive beta above critical limits.

Equation (3) along with the assumption that $\tau_{ci} = \tau_{pi} \approx 4\tau_{ce}$ for the ion conduction and particle times, respectively, combine to give τ_E for the plasma simulations. Figure 3 depicts the time dependence of $T_{i,n,\alpha}$, $n_{i,e}$, and β_θ for an ohmically-heated startup using the more pessimistic transport scaling given in Eq. (3). Ohmically-heated ignition with ν as low as 0.8 are computed as possible, ignition at lower values of the current exponent being possible only for plasmas of reduced size, higher current density, and increased power density. The sample simulation given in Fig. 3 assumes $T(r) = J_0(\mu r)$ and $n(r) = J_0(\mu r)$ profiles [i.e. $p(r) = J_0^2(\mu r)$, as dictated by the BFM], with a continuous fueling algorithm that holds I/N constant and always maintains the fueling rate below 1.3-1.4 times the maximum particle loss rate. The experimentally-determined[13] μ profiles (i.e., the "Best-Fit Model") are also used; these μ profiles correspond to a modified BFM with the $\mu(r)$ breakpoint, αr_p, being a specified function of θ. Figure 1 gives the F-θ diagram and startup trajectory for this sample case.

The time dependence of a range of confinement times, τ_j, during the plasma startup are also shown on Fig. 3, where j also includes the ohmic time [Eq. (2)] as well as classical cross-field ion conduction. At steady state the required τ_E is 6, 24, and 205 times less than Alcator, ohmic, and classical (ion) confinement times, respectively, τ_E being equal to ~ 50 Bohm times. If the more optimistic $\tau_{cc} \propto I_\phi^{3/2} r_p^2$ scaling is imposed, these margins are increased.

The TF and PF [composed of ohmic-heating (OH) and equilibrium-field (EF) coils] coil sets for the CRFPR are resistive (water-cooled copper) and must be sized and driven in a way that minimizes both the coil cost (mass) and (recirculating) power.[4] Figure 2 depicts such an optimized TFC/PFC set that also provides the optimal flux linkage, vertical field, and plasma magnetization.

Since the RFP plasma is heated and confined primarily by the self magnetic fields generated by a strong plasma current, I_ϕ, the PFC systems play a key role in the reactor design. The fundamental processes involved with an RFP startup are as follows. An initial toroidal bias field is produced by the TFC system. The plasma is initiated, and a changing PFC current induces the plasma current. The B_ϕ field is confined and compressed by the plasma, while the TFC current is reduced and ultimately reversed, achieving the RFP configuration [$B_\phi = J_0(\mu r)$, $B_\theta = J_1(\mu r)$]. The bulk of the toroidal-field energy is then provided by the plasma dynamo through the dominant PFC system. Having first achieved an initial, low-energy RFP state, the plasma dynamo would be used to increase further the toroidal field internal to the plasma. Raising the plasma current, the near-minimum-energy RFP state is maintained as turbulent plasma processes convert toroidal plasma current into poloidal current, which in turn increases the toroidal field trapped within the plasma column as F and θ remain constant near the minimum-energy state (Fig. 1). Sizing the TFC system to produce an initial field that is equal and opposite to the required (final) reversed toroidal field, the RFP configuration would be established at approximately 15-20% of the final plasma current for a Reversal Parameter in the range $F = -(0.15\text{-}0.2)$. The TFC system under these conditions requires two orders of magnitude less energy than the PFC circuit. Furthermore, the TFC set need not be designed for the startup overload, resulting in coils that dominate the PFC even less and leading to a more easily maintained system (Sec. IV).

The PFC set represents the dominant magnet system. Energy would be transferred to the PFC directly from the electrical grid. The simple circuit depicted in Fig. 4 is based on a bipolar operation that minimizes both forces and stored energy. The contribution of the EFC to the startup flux swing is minimized in order to maximize the bipolar operation, although this issue becomes less important if steady-state current drive (Sec. III.B.) proves feasible. Long-pulsed or steady-state operation also allows the OHC energy to transfer to the plasma through a resistive rather than through the capacitive element depicted on Fig. 4; the latter approach requires the temporary storage of ~ 50% of the transferred energy and adds to the total plant cost.

The RFP startup is based on a resistive transfer that crowbars the OHC while simultaneously initiating the plasma and connecting the EFC across the OHC circuit; an energy approximately equal to half the stored energy is transferred to the plasma, with an equivalent energy being dissipated in the transfer resistor. After the resistive transfer of the PFC current, the plasma current is 50-70% of the design (ignition) value; electrical grid power is then used to complete the trajectory towards full plasma current and ignition. Rapid initial current transients, limited only by the voltage allowed on the PFC system, can be achieved by the resistive transfer scheme. Since the transfer resistor has no inherent power-handling limitations, large plasma initiation powers can be generated without requiring either expensive on-site power-handling or energy-storage equipment; simultaneously, large transients on the electrical grid are avoided. The plasma and PFC (OHC + EFC + plasma) currents, voltages, and power transients during startup are also described in Fig. 4, which provides the electrical counterpart to Fig. 3.

B. Current Drive

Once a volt-second limit is reached on the inductive circuit depicted in Fig. 4, the plasma current would decay with a characteristic L_p/R_p time constant, which for the design-point parameters listed in Table II is 150-200 s. For the more realistic plasma profiles used in the time-dependent simulations, an energy of 1.2 GJ is stored in the poloidal field, which for peaked density and temperature profiles gives $I_\phi^2 R_p$ = 20 MW (5.1 MW for flat temperature profiles) and L_p/R_p = 120 s. Since the toroidal voltage applied to the ignited plasma is $\lesssim$ 1.0 V and to achieve ignition the plasma requires $\lesssim$ 190 volt-seconds, some extension of the CRFPR burn solely by inductive means is possible, albeit at higher voltages and currents in the PFC set. It is noted that the magnetic energy replacement time, W_M/P_E, is only a few seconds, where W_M is the total field energy and P_{ET} is the gross electric power; magnetic energy storage/recycle is not necessary for such extended burns. Nevertheless, the desire to minimize pulsed startup loads on the grid as well as mechanical/thermal stresses generated within the coils, blanket, and in-vacuum components, gives steady-state current drive a great attraction. Furthermore, the more pessimistic transport scaling ($\tau_E \propto I_\phi r_p^2$) requires the expenditure of additional resistive volt-seconds to achieve an ohmically-heated ignition, again giving impetus for reducing the frequency of such plasma startups.

The RFP dynamo offers a possibility for efficient, non-inductive, current drive. The principle of current drive by "F-θ pumping" of toroidal current is illustrated using the (analytic) BFM; more exact RFP profiles are treated numerically in Ref. 6. Driving steady-state currents in RFPs by oscillating the PFC and TFC circuits was first suggested by Bevir[14] and subsequently subjected to more specific examination.[15,16] In maintaining the magnetic helicity, K, constant and the plasma magnetic energy, W_M, at a minimum, oscillations in externally applied voltages that, for instance, change the toroidal flux, ϕ, excite the plasma dynamo to generate the toroidal voltages and currents required to maintain the minimum-W_M, constant-K RFP state. Describing[15,16] the RFP plasma as an electrical circuit in terms of K, ϕ, and W_M, the following relationship between plasma variables (i.e., F and θ) and circuit parameters (i.e., inductances, resistances, currents, and voltages) results.

$$V_\phi = I_\phi R_p + \left(L_p + \frac{\theta}{2} L_p'\right) \dot{I}_\phi + \left[\frac{1 - F}{c\theta} - \frac{c\theta}{2L_o} L_p'\right] V_\theta , \quad (4)$$

where $L_p' = dL_p/d\theta$, $\dot{I}_\phi = dI_\phi/dt$, and $V_\theta = +\dot{\phi}$; adoption of a positive Faraday's law for the toroidal circuit is based upon a convention that orients ϕ in the same direction as I_ϕ. The plasma inductance, L_p, includes the poloidal field inductance, $L_{p\theta} = 2W_{M\theta}/I_\phi^2$, as well

as the energy needed to compress a uniform toroidal flux, ϕ, into the Bessel-Function distribution, $B_\theta = J_1(\mu r)$; as seen from the footnote to Table I, typically $L_p/L_{p\theta} = 1.3 - 1.4$ for the BFM.

Table II defines key plasma parameters and their relationship to F and θ for the constant-μ BFM. This circuit equation illustrates the strong non-linear coupling between the poloidal and toroidal circuit voltages, V_θ and V_ϕ, through the plasma dynamo with the result that a net (mean) toroidal current can be driven by an oscillating toroidal voltage which itself has a zero mean. This behavior results from plasma motion associated with the relaxation process, the currents actually being driven by $\langle \tilde{v} \times \tilde{B} \rangle$ forces. This process is most directly seen through the helicity,[16] which has the following time derivative for the BFM.

$$\dot{K} = 2\phi(V_\phi - I_\phi R_p) \quad . \tag{5}$$

If V_ϕ is oscillated such that $\langle V_\phi \rangle = 0$, then the time average of Eq. (5) with $\langle \dot{K} \rangle = 0$ gives,

$$\langle I_\phi R_p \rangle = \frac{\langle \phi V_\phi \rangle}{\langle \phi \rangle} \quad , \tag{6}$$

where it has been assumed that $\langle \phi I_\phi R_p \rangle = \langle \phi \rangle \langle I_\phi R_p \rangle$ (i.e., small flux and current oscillations, δI_ϕ and $\delta\phi$, about large mean values, $\langle I_\phi \rangle$ and $\langle \phi \rangle = \phi_o$). Equation (6) shows that the average resistive voltage drop can be maintained by a zero-mean toroidal voltage oscillation if V_ϕ is large when ϕ is also large. Specifically, V_ϕ should be large in the current direction when ϕ is large (positive voltage is worth more in presence of high flux),[16] and ϕ should be small when V_ϕ is of reversed sign that inhibits current flow. This behavior is best demonstrated by assuming the following driving functions

$$\phi = \phi_o - \delta\phi \sin \omega t \tag{7A}$$

$$(V_\theta = \dot{\phi} = \delta\phi\omega \cos \omega t)$$

$$V_\phi = \delta V_\phi \sin \omega t \quad . \tag{7B}$$

In this case $\delta\phi/\phi_o/\delta V_\phi I_\phi R_p) = -2$ for $\langle \dot{K} \rangle = 0$, which implies $\delta V_\phi I_\phi R_p \geq 20\text{-}40$ if the toroidal flux variation is held to $\leq 5\text{-}10\%$ of ϕ_o to minimize the trauma to the RFP state. Furthermore, the plasma is assumed to relax rapidly along the F-θ diagram as V_θ and V_ϕ are subjected to the out-of-phase oscillation, implying that ω is much greater than the relaxation time. Recent experiments[17] have shown the ability of the RFP to track the F-θ diagram when either V_θ or V_ϕ are subjected to 1,000 Hz oscillations, indicating both the robust nature of the RFP dynamo and the potential for steady-state current drive.

To assess the tradeoff between $\delta\phi/\phi_o$, $\delta V_\phi/I_\phi R_p$, ω, $\delta I_\phi/I_\phi$, the dissipative power $P_\Omega = P_\phi$ and P_θ, a measure of the current drive efficiency, $\langle I_\phi \rangle / P_\Omega$, and the energy stored in the current drive circuits, E_ϕ, Eq. (4) has been solved numerically for the BFM under the constraint that $\langle \dot{I}_\phi \rangle$ and $\langle \dot{K} \rangle$ are zero. The voltage drive given by Eq. (7) is used, and Table II lists the F and θ dependences of R_p and L_p, as dictated by the constant-μ BFM. The dependencies of $\delta I_\phi/\langle I_\phi \rangle$ and $\delta V_\phi/\langle I_\phi R_p \rangle$ on $\delta\phi/\phi_o$ are shown on Fig. 4 for the CRFPR operating conditions and a frequency of 50 Hz. Selecting $\delta\phi/\phi_o = 0.01$ yields a value of $\delta I_\phi/\langle I_\phi \rangle$ near the minimum value of 0.003; reduced $\delta V_\phi/\langle I_\phi R_p \rangle$ relative to the value at the $\delta I_\phi/\langle I_\phi \rangle$ minimum are possible if higher I_ϕ oscillations are tolerable. Table III gives the associated parameters for this current-drive design point. For this closely coupled system the dissipative power, $P_\Omega = 5.7$ MW, entirely supplies the plasma ohmic losses and give a current drive efficiency of $\langle I_\phi \rangle / P_\Omega = 3.2$ A/W, which will decrease by ~2 for an engineered current-drive system. The energy stored in the poloidal and toroidal current-drive circuits is 0.26 MJ.

C. Ash/Impurity Control

Both (poloidal) pumped limiters and (toroidal) magnetic divertors are being considered as impurity/ash control for the CRFPR. Because of the dominance of poloidal rather than toroidal fields in the RFP, the geometry for each ash/impurity control scheme is generally orthogonal to that being proposed for tokamaks. Pumped limiters have received the majority of attention to date,[6] but understanding of both within the context of the RFP is not sufficient to allow a choice to be made at present.

1. Pumped limiters. Tokamak edge-plasma models[18,19] have been modified to describe the low-q RFP configuration.[6] The bases of the RFP scrapeoff model are the one-dimensional (cross-field) steady-state heat and particle equations, which in turn are coupled to a neutral-atom transport and sputtering models. Because of the higher average first-wall power density expected for the compact reactor, a greater fraction of the first-wall area must serve a limiter function. In fact, the first-wall area (110 m^2) for the CRFPR is comparable to the Starfire limiter area area (~ 58 m^2) and would operate at comparable power densities (4-5 MW/m^2).

The dominant poloidal field at the scrapeoff favors a toroidal array of N_L poloidal limiters, allowing a field-line reconnection length, $L = \pi r_p / N_L q$, that is sufficiently long for adequate radial diffusion into the scrapeoff as edge-plasma particles follow high-pitch (low-q) field lines between intersecting limiter surfaces. Bohm-like radial diffusion is assumed and must be sufficiently rapid to reduce the concentration of heat flux onto the leading edge of the limiter while simultaneously allowing an acceptably large particle flux under the limiter. As for other limiter configurations,[18,19] a large fraction ($f_{RAD} > 0.9$) of the plasma energy loss must be shed as radiation in order to reduce the energy/particle load on the limiter surface. Following similar studies for tokamaks[18], an algorithm is used[6] that adjusts the shape of the limiter surface to meet specific design heat-flux constraints while varying key design and physics parameters (i.e., the number of limiters, the design heat flux, the scrapeoff thickness, the cross-field particle transport in the scrapeoff, the edge-plasma conditions, the recycle rate, etc.). Table III lists typical limiter parameters that result from this extensive parameter survey.[6]

The RFP limiter design algorithm also performs a sputtering estimate, but uncertainties in neutral-atom transport, edge-plasma conditions, and redeposition profiles make these erosion estimates unreliable. As for other concepts, large gross sputtering rates are predicted unless very low or very high edge-plasma temperatures are assumed and/or larger radiation fractions (i.e., radiating plasma mantles) can be sustained. Although serious, the erosion problem should not be more difficult for the compact approaches in that for similar edge-plasma temperatures, profiles, and impurity levels, the ratio of neutron to particle flux onto the first wall should be independent of concept; the sputter erosion "fluence" (i.e., mm) per unit neutron fluence (MW yr/m^2) for plasmas of similar nt_p is independent of plasma power density. If, however, the sputter erosion rates cannot be accommodated by redeposition, cannot be reduced by

enhanced radiative loss, or interfere with the plasma operation, efficient magnetic divertors may be necessary.

2. Magnetic Divertors Because of the premium placed on compactness and reduced TFC mass, the pumped limiter appears as a natural first choice for an impurity-control scheme. The uncertainties associated with pumped limiters, particularly with respect to sputter erosion and the potential for degraded plasma performance, may demand better plasma/wall isolation. Most magnetic divertor designs null and re-direct minority-field lines, which for the tokamak creates a preference for poloidal divertors. Working with the minority field minimizes adverse effects on beta, transport, and auxiliary coils (forces, stored energy, and power consumption). Those tokamaks that divert the majority field accept these problems in trade for elimination of interlocking coils. Since the minority field in the RFP is toroidal, the above-mentioned physics issues can be avoided without the encumbrances of interlocking coils. Furthermore, the compact reactor options also allow placement of the divertor coils close to the flux surface that is to be broken and diverted, leading to an increased efficiency not available to superconducting systems.

The simplest design of a toroidal-field divertor for an RFP is one which merely adds TFCs of the appropriate size and current to the main TFC set. The divertor must isolate the region of field-line contact with structural surfaces and provide an exit for plasma exhaust. This goal is accomplished with divertor coils of radius sufficiently large to encase the main TFC set. The current in the coil that pulls the toroidal field must be sufficiently large to cancel the field from the TFC set. Viewing the nulling coils in each of N_D toroidal divertors as a solenoid which must cancel the field from the N toroidal-field coils, the current, I_D, in each divertor is approximately related to the TFC current, I_{TF}, by $N_D I_D = - N I_{TF}$.

These simple divertor coils will null the toroidal field indiscriminately within the bore of the TFC set. A pair of coils that flank the divertor coils are introduced with a combined current equal in magnitude but opposite in sign to that in the divertor coil; these flanking coils localize the nulling effect of the divertor coils to within approximately the distance between the divertor coil and its flanking coils. The flanking coils afford only gross control of the location of the toroidal-field null and the size of the divertor channel. A more precise control of the toroidal extent of the null is necessary to reduce the TFC perturbation by the divertor channel, the size of the first-wall gap, and the amplitude of the toroidal ripple induced, the latter resulting in island formation that affects both transport and field reversal. A method of controlling the toroidal extent of the field null has been demonstrated, but quantitative estimates of the latter two effects have not yet been made.

Control of the toroidal extent of the field perturbation can be achieved by introducing another divertor-flanking-coil (DFC) set with less current than the main divertor coil set but located closer to the plasma edge; the DFCs are enclosed by the TFC set and have a smaller gap between the divertor and the DFCs. A divertor design with four toroidal divertors is shown in Fig. 6. The effect of the secondary DFC set is evident from the pinching of the diverted field lines near the plasma edge. The property of localizing the divertor action to the outboard side of the plasma is particularly attractive. A more compact divertor design is possible, this design yielding nearly the same diversion of field lines by forcing the diverting coil currents to return through the DFCs rather than through the inboard side of the torus.

IV. CONCLUSIONS

The three central plasma-engineering issues treated herein (transport/startup, current drive, and impurity/control) combined with the high-power-density, cost-optimized design point to determine in large part the TFC characteristics for the CRFPR. The high neutron and heat loads combine with the perceived requirement for a conducting shell near the RFP plasma to suggest a copper-alloy first-wall/limiter system. The thin (~ 0.6-m) high-power-density blanket (~ 200 MW/m^3 peak, 30-40 MW/m^3 average) and shield (~ 0.1 m) combined with the relatively low magnetic field (< 3 T) at that position to make flowing liquid-metal breeder/coolant (PbLi alloy) particularly attractive.[3,6,20] The above considerations have led to the CRFPR cross-section given in Fig. 2 upon which a more detailed TFC engineering integration study is proceeding.[6] This design work is based upon the more space-conservative pumped-limiter impurity/control scheme, although toroidal-field magnetic divertors will also be considered once they are better understood in the context of the RFP geometry. This paper concludes with a brief description of the TFC integration and design approach.

The basic components of the ~ 1160-Tonne TFC are illustrated in Fig. 7. The relatively tight array of TFCs (~ 800 Tonne, total) allows straightforward access to the underlying TFCs (142 Tonne) and first-wall/blanket/shield (223 Tonne, including PbLi breeder/coolant) components only in the vicinity of the outboard equatorial plane through a ~ 1-m vertical gap provided in the TFC set. After lifting the top half of the TFC set (400 Tonne), the ~ 200-Tonne FW/B/S/TFC torus (drained of PbLi breeder/coolant) would be installed (removed) as a separate unit ("batch" maintenance); for purposes of off-site fabrication, however, this unit would be segmented into 24 toroidal sectors, each centered on a TFC.

The 24 poloidal limiter blades would be arrayed one per sector in the TFC midplane. The 30-40-mm limiter-blade standoff from the first-wall surface provides a total annular pumping area of 7-10 m^2 and covers ~ 25% of the FW, compared to 15 m^2 and ~ 7% for the Starfire tokamak.[7] Each of the 24 toroidal sectors contains two poloidal blanket sections with poloidally flowing PbLi breeder/coolant; each of these blanket sections is separated by a radially diverging vacuum-pumping slot that connects the backside of each limiter with a 70-mm vacuum plenum formed by the annulus defined by the blanket and shield. Adjacent shield segments are joined by an outer shell to provide structural unity to the FW/B/S torus, which again combines with the fixed TFC set to provide the single TFC maintenance unit. The low-field (≤ 1-T) TFCs are secured to this structure in order to react overturning and centering forces, and are self-supporting against outward radial forces. As seen from Fig. 7, square apertures are provided between TFCs at the outboard equatorial plane for both vacuum and PbLi ducting. Manifolds and mains to the water-cooled FW/limiter and shield components, as well as other utilities, are also provided in the outboard equatorial plane.

Electrical leads to the multi-turn TFCs and PFCs could be considerably reduced in size from the coils they drive. In order to maximize the coupling (i.e., minimize stray inductances), the low-current poloidal current-drive coils would be integral with the first-wall/limiter, whereas the required toroidal-field

oscillations would be provided by the existing TFCs.[21] It is noted that if F-θ pumping can be used to drive dc current in the CRFPR, the OHC set shown in Figs. 2 and 7 is needed only for startup. Considerable reduction in the size of the OHCs is expected, which in turn would also allow a reduced EFC set for the same cost and recirculating power fraction.

In summary, the characteristics of the key plasma engineering systems have been broadly described and quantified for the CRFPR. The operational and economic attraction of the compact approach may be attainable by the RFP, since it is one of a class of approaches that can confine plasma without the use of excessive toroidal fields. Furthermore, a potential exists for this confinement to be steady state. Maintenance of the regenerative dynamo action at higher plasma pressures while retaining the already reactor-relevant beta values with improved confinement times is central to achieving this ideal end-product and, therefore, represents the major experimental objective of the present RFP physics program.

REFERENCES

[1] R. Hancox, R. A. Krakowski, and W. R. Spears, Nucl. Eng. and Design 63, 2, 251 (1981).

[2] R. A. Krakowski and R. L. Hagenson, Nucl. Technol./Fusion 4, 1265 (1983).

[3] R. A. Krakowski, J. Nucl. Mater. (to be published, 1984).

[4] R. L. Hagenson and R. A. Krakowski, "Compact Reversed-Field Pinch Reactors (CRFPR): Sensitivity Study and Design-Point Determination," Los Alamos National Laboratory report LA-9389-MS (July 1982).

[5] R. A. Krakowski and R. L. Hagenson, Nucl. Technol./Fusion 4, 1284 (1983).

[6] R. A. Krakowski, et al., "Compact Reversed-Field Pinch Reactors (CRFPR): Preliminary Engineering Considerations," Los Alamos National Laboratory report (to be published).

[7] C. C. Baker (Principal Investigator), et al., "STARFIRE - A Commercial Tokamak Fusion Power Plant Study," Argonne National Laboratory report ANL/FPP-80-1 (September 1980).

[8] B. G. Logan, Nucl. Technol./Fusion 3, 563 (1983).

[9] J. B. Taylor, Phys. Rev. Lett. 33, 1139 (1974).

[10] H.A.B. Bodin and A. A. Newton, Nucl. Fus. 20, 1255 (1980).

[11] RFP Theory Workshop, Los Alamos National Laboratory, Los Alamos, NM (June 13-16, 1983).

[12] H.A.B. Bodin, "RFP Experiments - General," International Summer School of Plasma Physics, Varenna, Italy (September 7-17, 1983).

[13] K. F. Schoenberg, R. F. Gribble, J. A. Phillips, Nucl. Fusion 22, 11, 1433 (1982).

[14] M. K. Bevir and J. W. Gray, "Relaxation, Flux Consumption and Quasi Steady State Pinches," Proc. RFP Theory Workshop, Los Alamos, NM (April 28 - May 2, 1980).

[15] K. F. Schoenberg, D. A. Baker, and R. F. Gribble, Los Alamos National Laboratory report LA-9161-MS (1982).

[16] M. K. Bevir, J. G. Gimblett, and G. Miller, "Quasi Steady State Current Drive by Plasma Relaxations," Proc IAEA Technical Committee Meeting on Non-Inductive Current Drive in Tokamaks, Culham Laboratory, (April 18-21, 1983).

[17] K. F. Schoenberg, C. J. Buchenauer, R. S. Massey, J. G. Melton, R. W. Moses, Jr., R. A. Nebel, and J. A. Phillips, (submitted to Phys. Fluids, 1983).

[18] M. Ulrickson, "Optimum Shapes for Pumped Limiters," Princeton Plasma Physics Laboratory report PPPL-1901 (May 1982).

[19] H. C. Howe, "Physics Considerations for FED Limiter," Oak Ridge National Laboratory report ORNL/TM-703 (1982).

[20] M. E. Battat, R. J. LaBauve, R. A. Krakowski," Trans. Amer. Nucl. Soc. 44, 147 (1983).

[21] K. F. Schoenberg and R. F. Gribble, private communication, Los Alamos National Laboratory (1983).

TABLE I. ENGINEERING PARAMETER COMPARISON BETWEEN MAINLINE AND COMPACT RFP REACTOR DESIGNS[a]

	STARFIRE[7]	MARS[8]	CRFPR[5,6]
Gross thermal power (MWt)	4000.	3400.	3389.
Recirculating power fraction	0.167	0.22	0.16
Net electric power (MWe)	1200.	1202.	1000.
First-wall radius (m)	2.83[b]	0.60	0.75
Major radius (m)	7.0	131/214[c]	3.8
Plasma volume (m^3)	781.	98.8	37.7
Average beta	0.067	0.28	0.20
First-wall neutron loading (MW/m^2)	3.6	4.3	19.5
FPC mass (Tonne)	23,174.	23,308.	1,160.
FPC mass utilization (Tonne/MWt)	5.7	6.8	0.4
FPC power density (MWt/m^3)	0.5	0.29	14.0
FPC unit cost ($/kg)	19.0	20.5	37.0
(M/m^3)	0.053	0.041	0.20
(M/m^2)	0.66	0.97	0.36
RPE(Account 22)/TDC	0.56	0.64	0.36
Unit direct cost ($/kWe)	1439.	~~3400.~~ 1480.	863.
Cost of electricity (mills/kWeh)	67.	TBD	40.7

(a) The following abbreviations are used in this table: Fusion Power Core (FPC), Reactor Plant Equipment (RPE), Total Direct Cost (TDC), To Be Determined (TBD).

(b) Average value.

(c) Central-cell/total length including end cells and direct collectors.

TABLE II. CRFPR PLASMA AND CIRCUIT PARAMETERS FOR A 1000-MWe(net) MINIMUM-COE DESIGN POINT GIVEN ON TABLE I AND FIG. 1.[a]

PLASMA PARAMETER	VALUE
Minor plasma radius, r_p(m)	0.71
Major plasma radius, R_T(m)	3.8
Inverse plasma aspect ratio, $\epsilon = r_p/R_T$	0.19
Average plasma temperature, T(keV)	20[flat][b]
Average plasma density, $n(10^{20}/m^3)$	$5[J_0^2(\mu r)]$[b]
Toroidal plasma current, I_ϕ(MA)	18.5
Energy confinement time, τ_E(s)	0.23
F-θ model [$F = \theta J_0(2\theta)/J_1(2\theta)$]	BFM[b]
Pinch parameter, $\theta = B_\theta(r_w)/\langle B_\phi \rangle$	1.2-1.4
Reversal parameter, $F = B_\phi(r_w)/\langle B_\phi \rangle$	0.0-(-0.6)
Poloidal beta, β_θ	0.2
Streaming parameter, $I_\phi/N(10^{-14}$A m)	5.8
Classical plasma resistivity, $\langle\eta\rangle$ $(10^{-10}$ohm m)	3.4
CIRCUIT PARAMETERS	
Toroidal plasma inductance, $L_o(H) = \mu_o R_T \epsilon^2/2$	$8.3(10)^{-8}$
Poloidal plasma inductance, $L_{p\theta}(H) = (L_o/\epsilon^2)[1 + (F/\theta^2)(F - 1)]$	$(2.4\text{-}3.6)(10)^{-6}$
Plasma inductance[c], $L_p(H) = (2L_o/\epsilon^2)[1 + (2F + 1)(F - 1)/2\theta^2]$	$(3.1\text{-}5.1)(10)^{-6}$
Toroidal flux, ϕ(Wb) = $L_o I_\phi/c\theta$	5.9-6.9
"Screw-up" factor[d], g_{OHM} = $2(\theta^2 + F^2) - F$	2.9-3.0
Plasma resistance, R_p(ohm) = $2g_{OHM}\langle\eta\rangle/\epsilon^2 R_T$	$1.5(10)^{-8}$
Plasma poloidal flux, $L_p I_\phi$ (Wb)	44-66
Plasma ohmic voltage, $V_\phi(V) = I_\phi R_p$	0.3
Plasma decay time, L_p/R_p(s)	164-234

[a] The BFM is used here, whereas plasma simulations use the "Best Fit Model" (ref: Fig. 1 and text).

[b] The BFM requires a $J_0^2(\mu r)$ pressure profile.

[c] Includes compressional energy of an initially uniform toroidal flux.

[d] Based on a uniform temperature profile.

TABLE III. TYPICAL (F-Θ PUMPING) CURRENT-DRIVE PARAMETERS

PARAMETER	VALUE
Fractional Flux Swing, $\delta\phi/\langle\phi\rangle$	0.01
Voltage Swing, $\delta V_\phi/\langle I_\phi R_p\rangle$	200
Toroidal Voltage, $\langle I_\phi R_p\rangle$ (V)	0.31
Current Swing, $\delta I_\phi/\langle I_\phi\rangle$	0.004
Current Swing, δI_ϕ (MA)	0.078
Frequency, ω (Hz)	50
Dissipative Power, P^* (MW)	5.74
Poloidal, P^*_θ (MW)	3.44
Toroidal, P^*_ϕ (MW)	2.30
Efficiency Factor, $\langle I_\phi\rangle/P^*$ (A/W)	3.2
Stored Energy, E_ϕ (MJ)	0.26

TABLE IV. TYPICAL PUMPED-LIMITER PARAMETERS

Fraction of plasma energy lost by radiation	0.9
Edge-plasma recycle coefficient	0.8
Design heat flux (MW/m^2)	6.0
Edge-plasma temperature (eV)	33.
Edge-plasma ion density ($10^{20}/m^3$)	2.0
Number of limiters	24
First-wall minor radius (m)	0.75
Limiter coverage fraction	0.25
Limiter toroidal extent (m)	0.25
Limiter radial extent (m)	~ 40
Limiter thickness (mm)	~ 8-10
Fraction particles under limiter	0.37

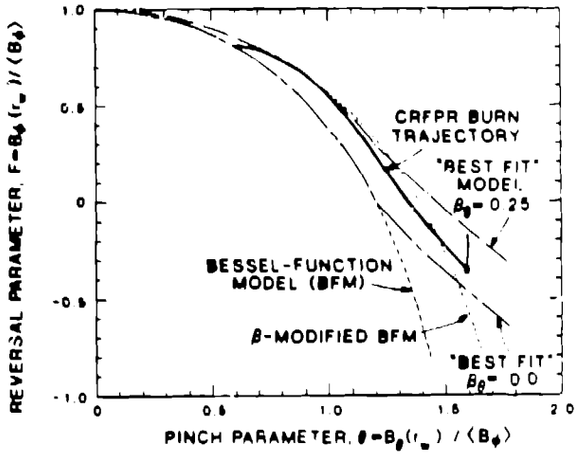

Fig. 1. RFP minimum-energy diagram.

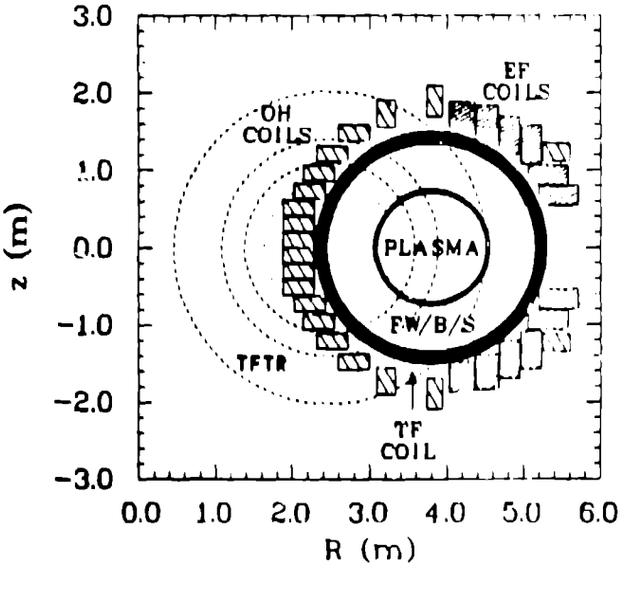

Fig. 2. CRFPR cross-section compared to TFTR.

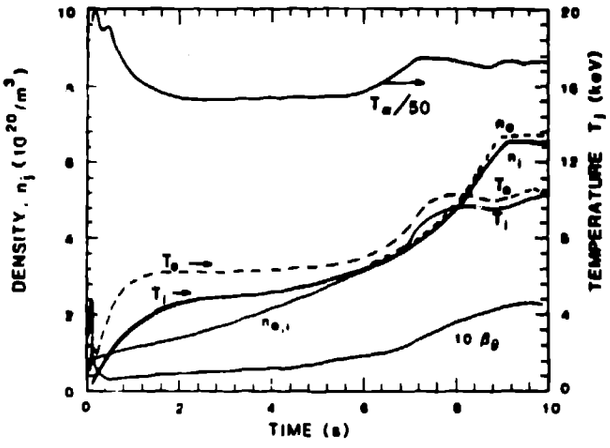

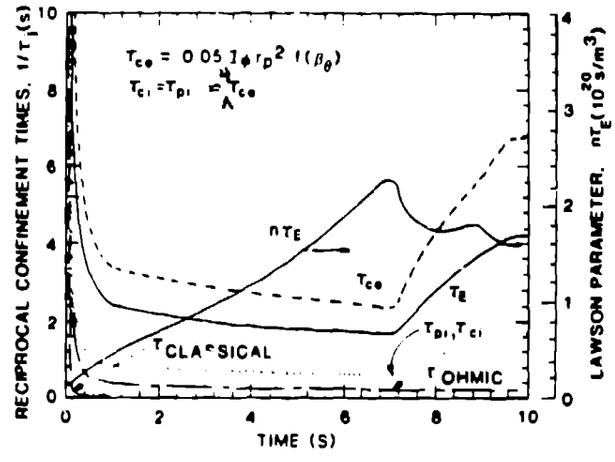

Fig. 3. Plasma parameters during startup.

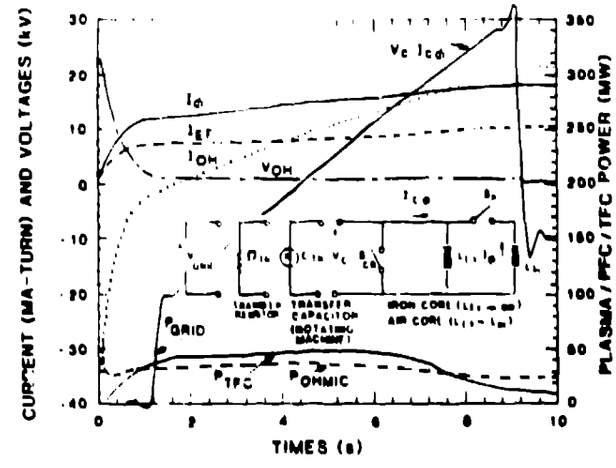

Fig. 4. Circuit transient during startup.

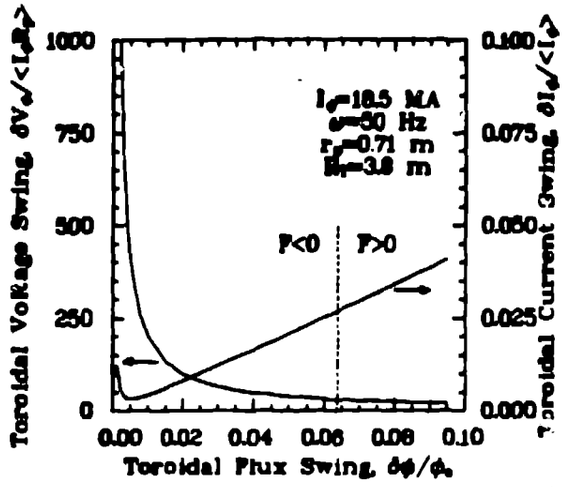

Fig. 5. Circuit/plasma options for "F-θ pumping" current drive.

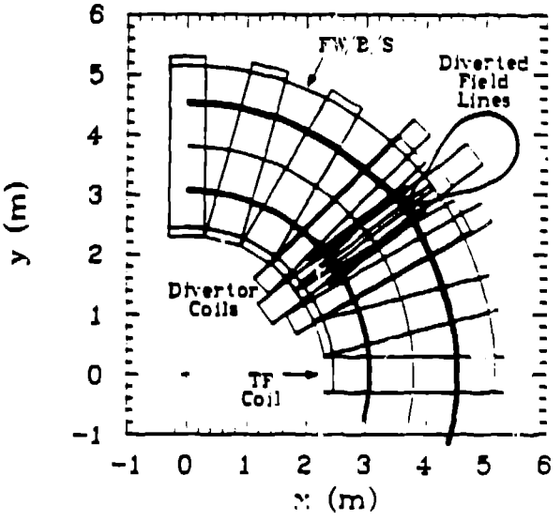

Fig. 6. Toroidal-field divertor.

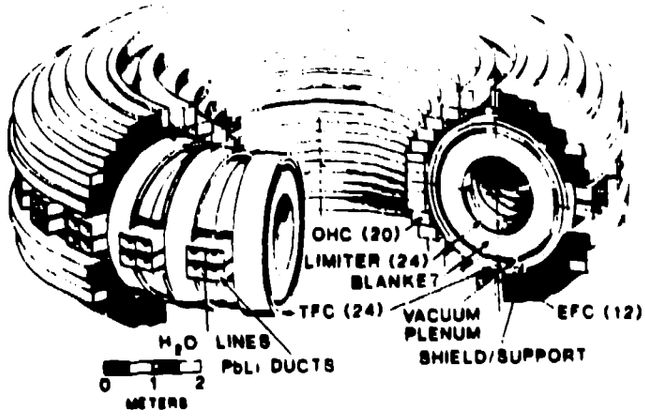

Fig. 7. Compact RFP reactor FPC integration (1,160 Tonnes).